Global Diversity of Mesopelagic Mesozooplankton

Yulia Egorova

yulia.egorova@ubc.ca

University of British COlumbia https://orcid.org/0000-0002-8712-7789

Gabriel Reygondeau

William Cheung

University of British Columbia https://orcid.org/0000-0001-9998-0384

Evgeny Pakhomov

University of British Columbia

Article

Keywords: twilight zone, species distribution models, mesozooplankton, diversity, rarity, latitudinal gradients, biodiversity

Posted Date: August 13th, 2024

DOI: https://doi.org/10.21203/rs.3.rs-4791399/v1

Additional Declarations: There is **NO** Competing Interest.

Title: Global Diversity of Mesopelagic Mesozooplankton

Authors:

Yulia Egorova[a*], Gabriel Reygondeau[b], William W.L. Cheung[c], Evgeny A. Pakhomov[a,c]

***Corresponding Author:**

Yulia Egorova, yulia.egorova@ubc.ca

The author's institutional affiliations:

[a] Department of Earth, Ocean, and Atmospheric Sciences, University of British Columbia, 2207 Main Mall, Vancouver, British Columbia, Canada

[b] Rosenstiel School of Marine, Atmospheric, and Earth Science, University of Miami, 4600 Rickenbacker Causeway, Miami, Florida, USA

[c] Institute for the Oceans and Fisheries, University of British Columbia, 2202 Main Mall, Vancouver, British Columbia, Canada

Emails:

yulia.egorova@ubc.ca

gabriel.reygondeau@miami.edu

w.cheung@oceans.ubc.ca

epakhomov@eoas.ubc.ca and e.pakhomov@oceans.ubc.ca

Abstract

Despite the ecological importance of mesozooplankton, little is known about their global distribution and diversity in the mesopelagic realm. This study examines the spatial distribution and diversity of 861 mesozooplankton species using species distribution models. The highest species richness and range-size rarity were found in the offshore North Atlantic and coastal areas across both hemispheres, while the Pacific and Indian ocean basins had low rarity and species richness. Latitudinal species richness peaks around 30° N and 30° S, with hotspots mainly within 40°S and 40°N, absent in polar areas. However, mean species richness per area is higher and more evenly distributed in polar regions compared to equatorial or tropical areas. The study also found a correlation between water temperature and species richness, with the highest richness at around 25°C, decreasing sharply below ~10°C.

Keywords

twilight zone, species distribution models, mesozooplankton, diversity, rarity, latitudinal gradients, biodiversity

Main Text

Introduction

Marine ecosystems are characterized by remarkable biodiversity, with 28 animal phyla, including 13 that are endemic to these environments[1]. Ocean supports over 2.2 million eukaryotes[2] with only around 10% of the species being described[3]. In comparison, terrestrial systems house only 11 phyla, with one endemic phylum. The drivers of such biodiversity vary across taxa and habitats, with temperature notably having a consistent association with biodiversity in the upper ocean layers[4] and a more complex relationship in a deep ocean[5].

Zooplankton, ranging from unicellular organisms to multicellular colonies larger than whales, inhabit oceans worldwide, from the poles to the deepest trenches. About 7,000 described species span nearly all animal phyla[6]. Most zooplankton fall within the size range of less than 1 mm to 1 cm, with copepods constituting 80-90% of the total zooplankton abundance in most marine ecosystems[1]. Mesozooplankton, in the size range of 0.2-20 mm, play a crucial role in carbon and nutrient cycling, transferring energy to the deep ocean[7,8].

The examination of broad-scale patterns in marine biodiversity is not straightforward due to the diverse scales at which organisms operate, from microns for microbes to entire ocean basins for migratory fishes and marine mammals. Therefore, the assessment of biodiversity gradients employs a taxonomic or habitat framework depending on the taxa involved. Mesopelagic organisms, found in the middle layer of the ocean, remain significantly understudied despite their pivotal role in oceanic carbon and nutrient cycling[9]. Despite the ecological importance of mesozooplankton, little is known about their global distribution and diversity in the mesopelagic realm[10].

Biodiversity can be measured in many ways[11]. Species richness, representing the total number of different species in a community, provides us with a snapshot of the complexity of the mesopelagic ecosystem[12]. Meanwhile, species range-size rarity offers an assessment of the relative abundance of less common or rare species, a significant yet often overlooked aspect of biodiversity[13]. Together, these measures present a more nuanced understanding of community structure and diversity.

Recently, a few studies looked at the global protozoan or metazoan diversity and their associated biomass[14,15]. Yet, our understanding of the global distribution and diversity of mesopelagic mesozooplankton (MM) remains incomplete. Furthermore, new insights from DNA-based techniques revealed previously unrecognized cryptic species, suggesting that current biodiversity may be severe underestimated[16,17]. There is a general paucity of studies looking at the global patterns of marine plankton diversity[4,18–20] with majority exploring particular taxa[21–24] often regionally and/or generally focused on epipelagic species[25–30].

The effort to create global distribution maps for major taxonomic groups is ongoing but hindered by insufficient sampling in many areas[31]. Given the significance of mesozooplankton in oceanic processes, estimating their global abundance becomes essential for modeling ocean biomass, biodiversity, and climate change[32]. These organisms show specific environmental preferences and tolerances, with some species residing in particular regional habitats and others having a broader distribution. The search for patterns in zooplankton distribution over the past century has revealed a few broad patterns[33]. The diversity in offshore habitats exceeds that in coastal regions, although

coastal biomass may be higher, and diversity generally increases from the poles to the tropics with a dip in an equatorial area[34]. With increasing depth in polar systems diversity has a mid depth peak in temperate/subarctic systems, but may peak in surface waters of tropical oceans[35]. However, these patterns vary among different taxonomic groups.

This study aimed for the first time to understand the spatial distribution and diversity of MM in the global ocean. It focused on two objectives (a) to estimate regional and global diversity patterns of MM with the highest precision possible and (b) to identify regional and global patterns and drivers of species richness and rarity. Our findings aimed to provide crucial insights into ecological roles and evolutionary histories of these organisms, enabling more informed conservation strategies and potentially revealing their importance in global biogeochemical cycles.

Methods

Utilizing the Mesopelagic Mesozooplankton and Micronekton Database[5] (MMMD), 861 species of mesozooplankton and micronekton in the mesopelagic zone were identified and reconciled with the World Register of Marine Species[3] (WoRMS). Synonyms and traits of species habitat were compiled from SeaLifeBase[36] (www.sealifebase.org). Species distribution records were gathered from the Ocean Biogeographic Information System (OBIS, http://iobis.org, accessed June 2022), which were integrated with records from synonym names and additional data from the MMMD. Environmental data considered for species bioclimatic envelopes included water temperature, salinity, dissolved oxygen concentration and nitrate concentration at the mesopelagic depth, mixed layer depth, net primary production, and euphotic zone depth (Table S1). Distributions of environmental variables are shown in Fig. S1. The data, sourced from the World Ocean Atlas 2018, NASA MODIS, and GDFL ES2M model, were interpolated to an equal-area grid with a per cell area of 3091 km^2. Specific modeling procedures follow the method described in Reygondeau[37] while the full method for MM is described in Egorova[5].

An ensemble forecasting approach was employed to model species' climatic envelope, which improves the robustness of forecast abilities. Eight different modelling algorithms were amalgamated into a weighted ensemble model: generalized linear models (GLM), generalized additive models (GAM), random forests (RF), artificial neural networks (ANN), flexible discriminant analysis (FDA), classification tree analysis (CTA), surface range envelope (SRE or BIOCLIM), and maximum entropy modelling (MAXENT). We used weighted mean approach, where a superior model is given stronger weight. TSS and AUC evaluation statistics were used to weight the models, with only robust individual models (those with AUC scores above 0.6) included in ensemble models.

The habitat suitability index (HSI) was computed for each species using weighted averages. HSI has a scale of 0 to 1000 (where 0 refers to low suitability and 1000 to high suitability areas). Binary (modelled presence/absence) outputs were generated from the AUC threshold value of the ROC using the Youden index[38]. This index maximizes the sum of sensitivity and specificity, and graphically can be represented as the maximum vertical distance between the ROC curve and the diagonal line. If the HSI was greater than or equal to the threshold, then the species were considered present. Species richness was subsequently computed by summing the number of species present in each grid cell.

Additionally, we computed two metrics of rarity for each cell: total range-size and average range-size rarities. Total range-size rarity, also known as endemism richness[13] or weighted endemism[39], was calculated as a sum of the inverse range-sizes for each cell[40]. Average range-size rarity, also known as corrected weighted endemism[39], was calculated as total range-size rarity divided by the number of species in the cell. For each map of species richness and rarity, the latitudinal diversity gradient (LDG) was computed (along with a mean and maximum number of unique species per latitudinal degree). Global patterns of species diversity and endemism, represented by species richness and total range rarity, respectively, were mapped. We subsequently related natural logarithms of the mesopelagic species richness with average water temperature in the mesopelagic layer and the inverse of thermal energy. Inverse thermal energy was calculated using $1/kT$ formula, where k is Boltzmann's constant and T is temperature in Kelvin.

Results

The species richness map constructed using the weighted mean ensemble model (Fig. 1A) showed the highest diversity in the North Atlantic between 30 and 40°N band, in near-shore areas, and in the Mediterranean Sea. Equatorial areas had moderate species richness. Areas of low diversity spatially coincided with all basins of the Pacific, South Atlantic, Indian oceans and circumglobal Subtropical Front. The Arctic Ocean showed uniformly moderate species richness values while those in the Southern Ocean varied between areas. The most extreme latitudes where species richness was observed extended up to 75.8°S in the southern hemisphere and 80.3°N in the northern hemisphere (Fig. 1B).

Predicted 'hotspots' of species richness (high number of species per cell) were primarily found in cells between 40°S and 40°N with the highest values in species richness found around 30° latitudes (Fig. 1B). At high latitudes, the maximum species richness per cell did not exceed 200 in the Southern Hemisphere and less than 300 species in Northern Hemisphere. However, species richness in areas between 30°S and 30°N was non-uniform and varied drastically depending on the cell location. In contrast, at high latitudes, the variability in species richness values was five orders of magnitude lower. As a result, although no species richness hotspots were found in polar areas (areas higher than 65.5° latitude), the number of species per cell was more uniform. Thus, when looking at mean species richness values per degree latitude (black line in Fig. 1B), polar areas have on average higher mean species richness per cell than any equatorial or tropical areas, however the highest mean species richness was found at approximately 40°N.

When all 861 species were used to calculate total and average- range size rarities, an unexpected pattern of high rarity values were found at the eastern side of the South Pacific gyre (Fig. S2). Closer examination of the area showed that the high rarity score (especially for average rarity) resulted from the presence of two crustacean species *Allosergestes pestafer* and *Echinomysis serratus*. *A. pestafer* was a formally known as *Sergestes pestafer*[41] received its new taxonomic genus in 2008[42], and its occurrence records are restricted to the eastern part of the South Pacific gyre and likely had a narrow environmental envelope due to a narrow environmental sampling. Since during the species distribution modeling (SDM) process the distribution of species is determined by the set of environmental conditions (specifically mixed layer depth), the SDM could predict the occurrence of *A. pestafer* only in a specified area. A similar effect of environmental variables on *E. serratus* prediction has also contributed to the observed anomaly. Based on the above, we decided to omit these species in calculations of rarity scores.

There were seven outlier cells with high total range-size rarity scores (>0.97) in the North Atlantic along the east coast of Canada (Fig. S2 at ~ 40°N). It can be explained by the presence of *Unciola irrorata* only in those cells which made the rarity of those cells extremely high. To better see the patterns of total rarity and their LDG, we filtered out the total rarity greater than 0.97 to remove the points with high rarity. When outliers were removed, that pattern in total range-size rarity became more evident: high values were found in pelagic areas closest to coasts, in the North Atlantic and Mediterranean Sea (Fig. S3). In general, total rarity was higher in polar areas of the Northern Hemisphere than in the Southern Hemisphere. Lowest rarity was observed in subtropical gyre regions of the Pacific, Indian and South Atlantic oceans. Total range-size rarity (Fig. 1D, Fig. S3) was generally higher towards the high latitudes of the Southern Hemisphere.

Total range-size rarity is correlated with species richness[43]. Hence, when corrected by a number of species in a cell, average range-size rarity showed a very biased outcome with a high rarity observed in the South Pacific gyre at 30°S (Fig. 1E) that can be explained by a very small sampling effort in that area (only 5-20 species are predicted within that region). Overall, the average rarity remained constant between 30°S and 30°N latitudes, while it increased towards the poles in both hemispheres. Highest average scores were found in the North Pacific in areas close to the coast. The North Atlantic, Arctic and the Southern Oceans were areas with high species richness and rarity (Fig. 2). Almost the entire Pacific and center of the Indian Ocean were areas with low rarity and low species richness, except for the eastern part of the South Pacific gyre where low species richness and high average rarity were observed (Fig. 2B).

A common predictor of the diversity gradient, especially for ectothermic species, is temperature. We subsequently related mesopelagic species richness with average water temperature in the mesopelagic layer and the inverse of thermal energy (Fig. 3). In total, 81% of the cells have a mean temperature in mesopelagic zone varying between 5 and 19°C, 18% of cells had mean temperatures colder than 5°C, and only 1% of areas had temperatures higher than 19°C. Around 150 species per cell can be found at the coldest water temperatures, with species richness decreasing to its global minimum at around 10°C and then gradually increasing reaching maximum at approximately 20°C. However peak and decline at higher temperatures are not well established since very few data points were available at those temperature ranges. After closer inspection, we found that the dip at ~10°C was also characterized by very high variability in mean temperatures in those regions (Fig. S4).

Discussion

Several studies have explored global patterns of marine species diversity [4,18–20]. However, all these studies have focused either on the entire available diversity or only epipelagic species. This work is the first attempt to model individual species distributions in the mesopelagic realm using mesozooplankton fauna. Globally, approximately 7000 species of marine zooplankton, mostly holoplanktonic, have been identified and described to date [44]. However, the portion of organisms found in the mesopelagic realm is unknown. In this work, we are working with the smaller subset of 861 MM species representing only 12.3% of the total known zooplankton organisms. The chosen subset of species is unlikely to encompass all MM species because it is a challenge to classify a species as 'mesopelagic,' particularly in the absence of depth range information for many zooplankton species. Therefore, this work should be considered as a preliminary study that sets up new questions and encourages the ongoing enhancement of the database to support more comprehensive and detailed analyses in the future.

The majority of the modelled species were from the phylum Arthropoda (n=644) due to the large representation of copepods, and hence this pattern of observed species diversity and LDG was more representative of the arthropods than the entire mesopelagic community (Figs. S5-S11). The prevalence of arthropods in the dataset is not surprising as this phylum comprises 44 - 47% of total species diversity (0-5000 m depth range) in the Northwest Atlantic Ocean[45]. Members of this phylum also dominate the community density and biomass values in both epipelagic and mesopelagic layers[46–48].

Other taxa records are patchier and/or are absent from many regions (Figs. S5-S11) due to variable sampling efforts (Fig. S12). For instance, Chaetognatha records are sparse throughout the Pacific Ocean and South Atlantic (Fig. S7). More sampling is needed for Chordata (Fig. S8) and Mollusca (Fig. S11) in the center of ocean basins, especially given their importance for commercial activities. However, these taxa are generally more neritic with a lot of possibility of migration and movement making them harder to sample. In addition, very few species of mesopelagic jellyfish were available in MMMD (<0.08% of the records are from the depth deeper than 200 m) due to the difficulty to sample these taxa using conventional (net/trawls) methods without destroying them once brought to the surface. General under sampling of gelatinous zooplankton in the mesopelagic realm could not even been remediated by using the JeDI Database (https://www.bco-dmo.org/dataset/526852) and therefore there is a general lack of data on jellyfish diversity and depth distribution in our analysis. This is considered as one of the largest knowledge gaps because currently we know about the overwhelming dominance of gelatinous organisms in the deep ocean[49,50].

The construction of the species richness map even based on limited dataset using the weighted mean ensemble model revealed global patterns in zooplankton diversity (Fig. 1A). The highest diversity was observed in the North Atlantic region, north of the South American continent, along the west coast of India, and in the Mediterranean Sea. Elevated species richness values were also observed in equatorial regions as well as Arctic and Southern Oceans. Generally, a moderate species richness was observed in the Arctic Ocean and variable species richness values in the Southern Ocean. In contrast, low diversity hotspots were associated with all basins of the Pacific, South Atlantic, and Indian oceans, as well as at the circumglobal subtropical front, i.e., in high-nutrient, low-chlorophyll regions.

The LDG analysis identified species richness 'hotspots' (high number of species per cell) between 40°S and 40°N, with the highest values found in cells around the 30° latitudes (Fig. 1B). This appeared to be comparable to finding of Rogers *et al.*[51] and Chaudhary *et al.*[20] for the observed total metazoan diversity. The absence of species richness hotspots in polar areas is noteworthy and perhaps counterintuitive, because the latitudinal mean species richness in polar regions appeared to be higher than in equatorial or tropical regions, despite localized hotspots. Although this pattern can arise from various factors such as temperature regime, productivity, currents, and mesoscale features, it appears that polar regions tend to exhibit simpler and less variable species communities[52]. The harsh conditions prevalent in these regions likely support only a limited and relatively constant number of specialized species[52]. At the same time, warm and dynamic equatorial waters that likely favor a high species turnover rate inhabited by patchy communities of the low and high speciation. Lower mean species richness in equatorial waters is potentially a reflection of a prevalence of low speciation patches. It may indeed also be an artifact of sampling efforts and thus should be further investigated.

Mean species richness peaked at approximately 40°N (Fig. 1B), which may be attributed to several factors. This latitudinal band is a transition zone between colder, nutrient-rich, temperate, and warmer, nutrient-poor, subtropical waters allowing higher productivity that is able to support a wide range of zooplankton species. Furthermore, fronts are by definition mixing zones that harbor neighboring communities mechanically increasing biodiversity. Marine LDG displays a bimodal distribution with peaks of species richness located around 30° of latitude in both hemispheres and tailing off towards the poles (Fig. 1B). This result is also consistent with a previous review study that found bimodality in almost all global datasets of 65,000 recent and 50,000 fossil coastal marine species [20]. However, LDG for global phytoplankton richness[19] showed a unimodal pattern with a peak in the inner tropics (<5°N and S). Non-collocated species richness maxima between phytoplankton and zooplankton species were also recorded by Benedetti *et al.*[53].

Previous research has suggested that a bimodal species richness pattern in zooplankton could be explained by several factors. One potential explanation is a sampling bias, where a higher number of samples are available in the Northern Hemisphere compared to the Southern Hemisphere[54]. Another possibility is the effect of the continental shelf extent, with equatorial areas having less continental shelf area. Temperature may also be a contributing factor, as suggested in studies by Tittensor *et al.* [4] and Beaugrand *et al.*[55]. While it may be true, Chaudhary *et al.*[20] have demonstrated that even after correcting for the sampling bias, the bimodality persisted. In this analysis, we excluded areas of the continental shelf shallower than 200 m to avoid potential interference of the coastal environment with the mesopelagic community species richness analyses. In addition, temperature affect appeared to be unimportant in this analysis with euphotic depth, dissolved nitrate and salinity being primary drivers of the MM distribution (Egorova *et al*. submitted).

This study found that the total range-size rarity shows a similar pattern as species richness pattern, with high values found in the offshore North Atlantic and in coastal areas across both hemispheres (Fig. 1C). In general, total rarity was higher in polar areas with the highest values observed in the Northern Hemisphere. The lowest rarity was predicted in gyres of the Pacific Ocean. Notably, low rarity in gyres can indeed be explained by the sampling bias. Due to reduced sampling efforts, only a few species had been recorded from these areas while well mixed and uniform conditions within gyres may not be properly represented in SDMs. The underrepresentation became even more evident when we explored an outlier of the high average rarity in the South Pacific gyre at 30°S (Fig. 1E). After removing the outliers, the average size rarity showed a clearer pattern, with the lowest absolute rarity values observed in equatorial areas gradually increasing towards polar areas (Fig. S9).

Similar to total range-size rarity, average rarity was higher in the Arctic Ocean compared to the Southern Ocean (Fig. 1). The reason for the higher average rarity of zooplankton species in the Arctic compared to the Southern Ocean is not entirely clear and may be influenced by a range of factors. One possibility is that the Arctic has a more diverse range of habitats and niches than the Southern Ocean, which may support a greater diversity of rare and specialized species. Additionally, Arctic ecosystems while overall younger, maybe are more fragmented and isolated than those in the Southern Ocean, which could promote the development of unique and highly specialized species[56,57]. Our study thus suggests that patterns of rarity may be influenced by a range of factors, such as the diversity of habitats and niches, environmental conditions, and sampling efforts.

After combining two metrics: rarity and species richness, it was found that the North Atlantic, Arctic, and Southern Ocean are areas of high species richness and high rarity (Fig. 2). The Pacific and Indian ocean basins are areas with low rarity and low species richness. These patterns can be explained by the proximity of the points to the coast, as well as the low resolution used in the study. One possibility is that ocean basins are typically characterized by low productivity and nutrient availability, which can limit the diversity and density of species. Additionally, ocean basins are often vast and homogeneous in terms of environmental conditions, which can limit the development of specialized and unique species.

The evolutionary rates hypothesis states that high temperatures and UV radiation can increase the mutation rate of land plants, resulting in a faster evolutionary rates and speciation[58,59]. Therefore, regions with high levels of energy may be characterized by a greater diversity of species due to the accelerated evolutionary processes in those areas[60] demonstrated that the relationship between temperature and avifauna species richness typically follows a positive deaccelerating curve. Findings of this study showed a similar relationship when mesopelagic water temperature exceeded 10°C (Fig. 3). However, we also found a species richness minimum at ~10°C with species richness values increasing slightly when temperatures are colder. Similar dip in species richness was also observed in the phytoplankton diversity[19]. Complementary to Righetti *et al.*[61], three regimes across the mesopelagic ocean were identified: gradual decrease in species richness for temperatures below 10°C, steep increase is species richness for temperatures between 10 and 19°C, and more or less consistent high species richness for temperatures greater that 15°C with MM species richness reaching a maximum at water temperatures of ~20°C. Such warm mesopelagic temperatures found only in semi-enclosed mesopelagic basins (e.g., province 14-16 and 23, in Fig. D6) or areas closest to the coast in equatorial and tropical regions. However, we did not find good agreement with the metabolic theory of ecology that expect a linear relationship between the variables. It is because the majority of points located in areas with temperatures between 5 and 19°C, had a very pronounce V-shaped pattern similar to Righetti *et al.*[61]. We speculate that such suppression of species richness in intermediate temperatures can be due to the high variability of temperature in the mesopelagic zone (Fig. S11B). However, the underlying mechanism is not known and requires further investigation. There seems to be a similar relationship between species richness and temperature for both epipelagic and mesopelagic layers, indicating that there may be a unifying mechanism that established the species richness in the open pelagic ocean. Egorova *et al*. (submitted) have identified salinity, dissolved nitrate, dissolved oxygen and euphotic depth to be important variables driving the distribution of species. These variables are predicted to vary under climate change, so further work is needed to explore these drivers of species richness in mesopelagic ocean.

The validity of global diversity patterns found in this study can be a result of the robust modelling approach employed. For example, in the Atlantic Ocean northern and southern hemispheres were unevenly sampled. However, discovered macroecological patterns are symmetrical according to the equator. This is a testimony to the modelling approach employed because discovered patterns appear to hold at vastly different levels of the data coverage. While further model tunes up and data collection are required, employing this approach in regions with limited sampling would allow inferring true macroecological patterns in the world ocean. Overall, this study serves as a valuable starting point for predicting the distribution of marine species, and its findings can be used to inform conservation and management efforts in marine ecosystems. Yet, to fully understand the diversity and distribution of mesopelagic species and to address the discrepancies observed

between the different phyla a continued mesopelagic sampling effort including *in situ* imaging and genomics coupled with machine learning technologies are warranted.

Author contributions

Y.E., G.R., and E.P. conceived and designed the experiments. S.Y. performed all designs and experiments. Y.E. analyzed the data. All authors discussed the results and jointly wrote and commented on the manuscript.

Code availability

The data availability for this study is as follows: all additional information about a study can be found in the Supplementary Material. The scripts and data used in this study are all available online at https://github.com/yuliaUU/glob-diver-mesopel-zoop.

Figures

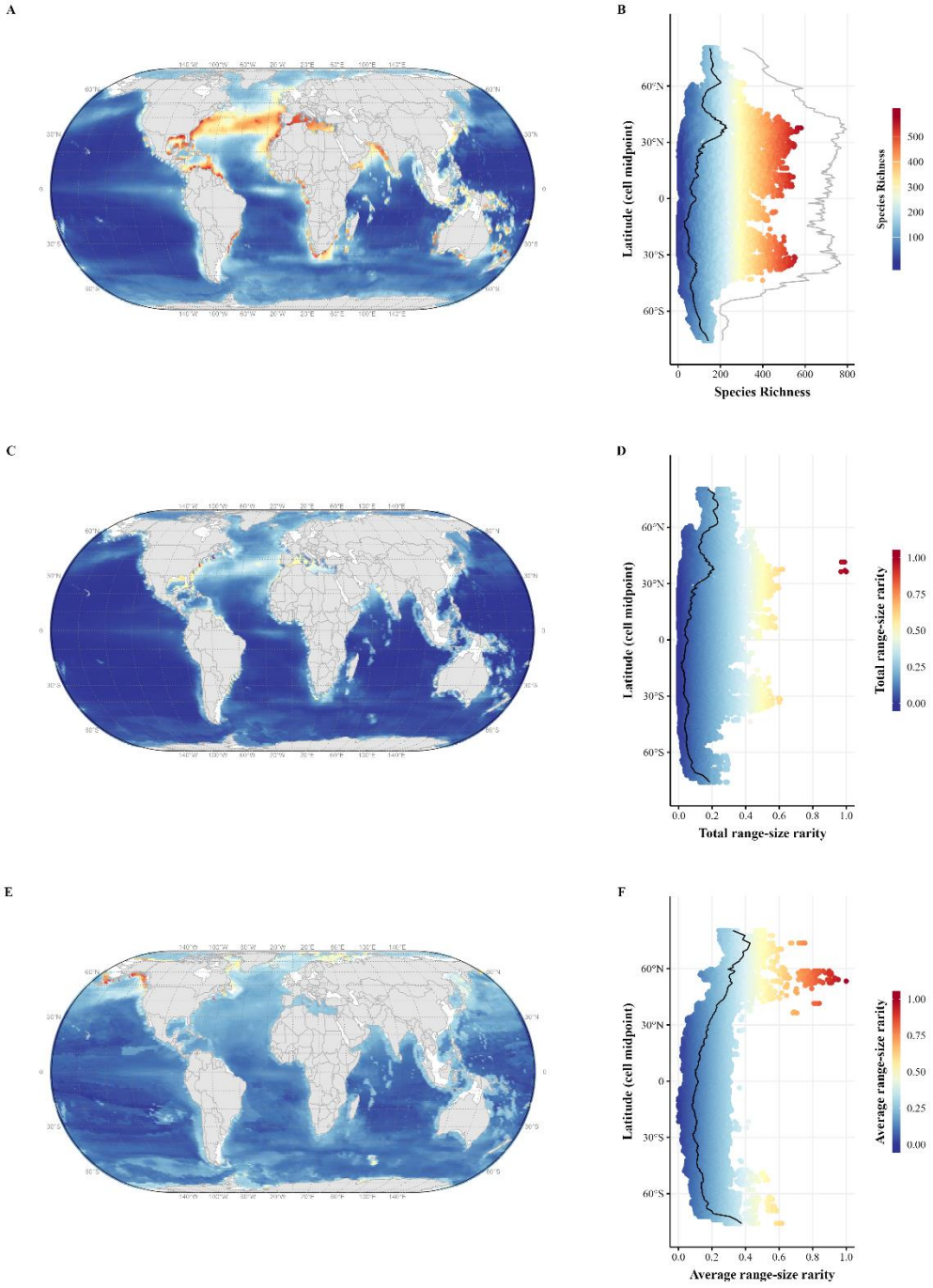

Figure 1: A) Mesopelagic mesozooplankton species richness map (n=859). B) Latitudinal gradient showing mean (solid black line) and a number of unique species (grey solid line) per latitude. C) Total range-size rarity map and D) latitudinal gradient for the total range-size rarity. A solid black line is a mean total range-size rarity per latitude. E) Average range-size rarity map and F) latitudinal gradient for the average range-size rarity. A solid black line is a mean total range-size rarity per latitude. All maps are in Eckert IV global equal area projection.

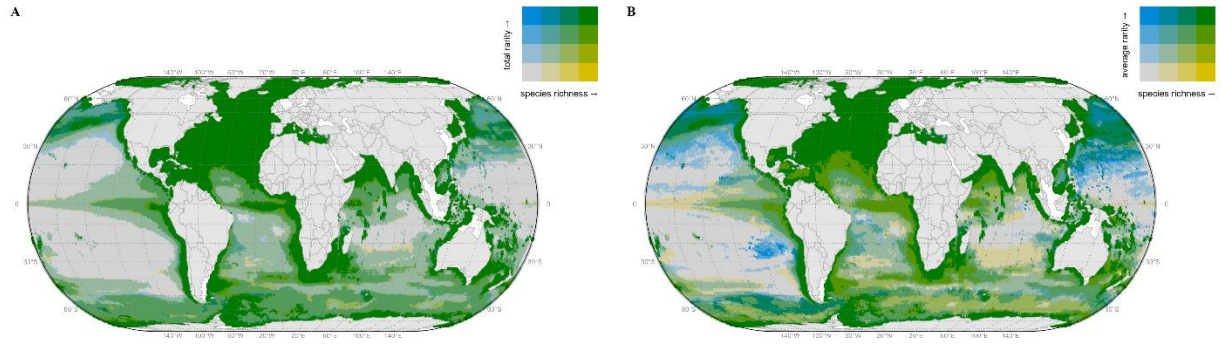

354

355 Figure 2: 2D map depicting the relationship between the species richness and A) total range-size
356 rarity and B) average range-size rarity. For both maps, quantile breaks were created at the 25th,
357 50th, and 75th percentiles. All maps are in Eckert IV global equal area projection.

358

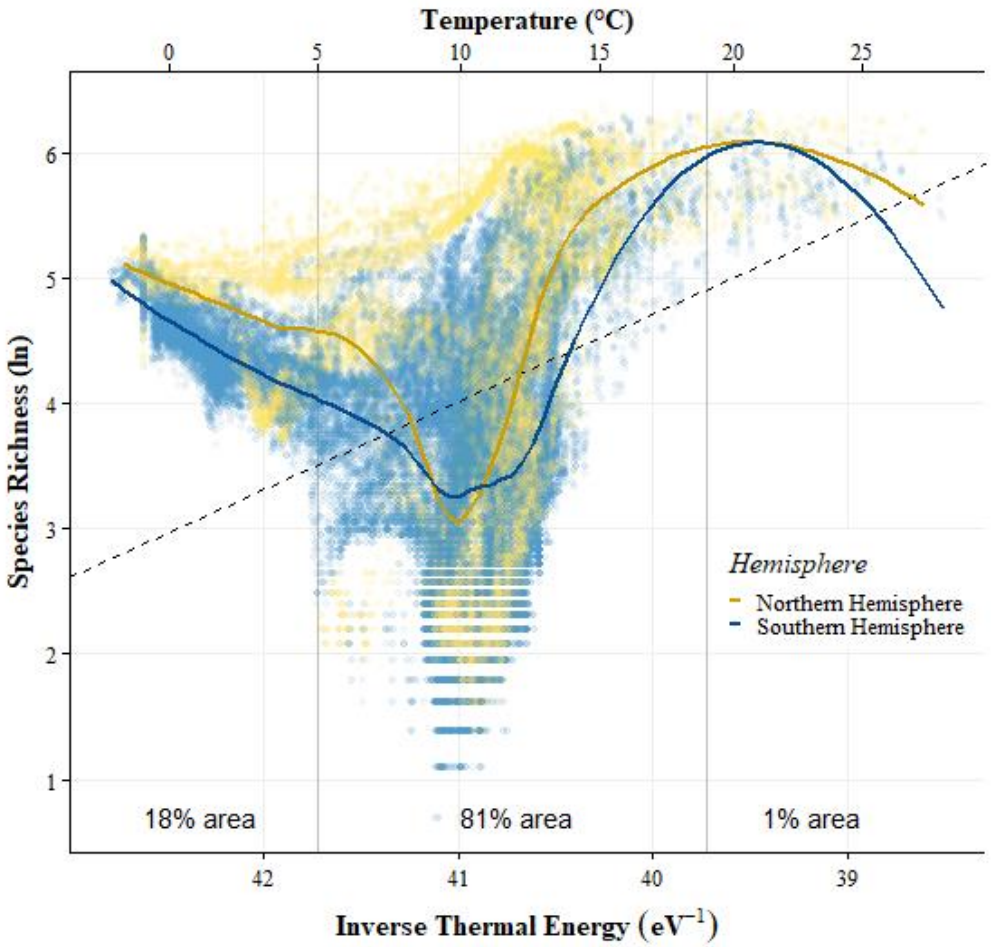

Figure 3: The natural logarithm of species richness as a function of water temperature (°C) in the mesopelagic zone and inverse thermal energy (1/kT, where k is Boltzmann's constant and T is temperature in Kelvin). Trendlines shown for each hemisphere (regressions with local polynomial fitting). Dashed black line represents the equation with slope -0.70 from metabolic theory from Brown *et al.*[62].

References

1. United Nations. The First Global Integrated Marine Assessment (World Ocean Assessment I), 2016.
2. Mora, C. *et al.* Global human footprint on the linkage between biodiversity and ecosystem functioning in reef fishes. *PLoS biology* **9,** e1000606; 10.1371/journal.pbio.1000606 (2011).
3. WoRMS Editorial Board. World Register of Marine Species. Available from https://www.marinespecies.org at VLIZ. Accessed 2023-06-07, 2022.
4. Tittensor, D. P. *et al.* Global patterns and predictors of marine biodiversity across taxa. *Nature* **466,** 1098–1101; 10.1038/nature09329 (2010).
5. Egorova, Y. Global distribution and biomass of the mesopelagic mesozooplankton and micronekton community. Doctoral dissertation. University of British columbia, 2023.
6. Wiebe, P. H. *et al.* Deep-sea sampling on CMarZ cruises in the Atlantic Ocean – an Introduction. *Deep Sea Research Part II: Topical Studies in Oceanography* **57,** 2157–2166; 10.1016/J.DSR2.2010.09.018 (2010).
7. Sutton, T. T. Vertical ecology of the pelagic ocean: classical patterns and new perspectives. Classical patterns and new perspectives. *Journal of fish biology* **83,** 1508–1527; 10.1111/jfb.12263 (2013).
8. Stemmann, L. *et al.* Global zoogeography of fragile macrozooplankton in the upper 100–1000 m inferred from the underwater video profiler. *ICES Journal of Marine Science* **65,** 433–442; 10.1093/icesjms/fsn010 (2008).
9. Béhagle, N. *et al.* (eds.). *Acoustics characterization of micronekton spatial distribution in Indian Ocean using scientific surveys and integrated marine observing system database: Acoustics characterization of micronekton* (IEEE, 2015).
10. Robinson, C. *et al.* Mesopelagic zone ecology and biogeochemistry – a synthesis. *Deep Sea Research Part II: Topical Studies in Oceanography* **57,** 1504–1518; 10.1016/j.dsr2.2010.02.018 (2010).
11. Yang, Q., Liu, G., Casazza, M., Gonella, F. & Yang, Z. Three dimensions of biodiversity: New perspectives and methods. *Ecological Indicators* **130,** 108099; 10.1016/j.ecolind.2021.108099 (2021).
12. Moore, J. C. Diversity, Taxonomic versus Functional. In *Encyclopedia of Biodiversity* (Elsevier2013), pp. 648–656.
13. Kier, G. & Barthlott, W. Measuring and mapping endemism and species richness: a new methodological approach and its application on the flora of Africa. *Biodiversity and Conservation* **10,** 1513–1529; 10.1023/A:1011812528849 (2001).
14. McIvor, I. A comparison of the geographical and vertical distribution of mesozooplankton communities from 0 to 1000 m at a global scale. MSc. University of British columbia, 2011.
15. Irigoien, X., Huisman, J. & Harris, R. P. Global biodiversity patterns of marine phytoplankton and zooplankton. *Nature* **429,** 863–867; 10.1038/nature02593 (2004).

16. Hebert, P. D. N., Cywinska, A., Ball, S. L. & deWaard, J. R. Biological identifications through DNA barcodes. *Proc. R. Soc. B* **270,** 313–321; 10.1098/rspb.2002.2218 (2003).

17. Mora, C., Tittensor, D. P., Adl, S., Simpson, A. G. B. & Worm, B. How many species are there on Earth and in the ocean? *PLoS biology* **9,** e1001127; 10.1371/journal.pbio.1001127 (2011).

18. Costello, M. J. & Chaudhary, C. Marine Biodiversity, Biogeography, Deep-Sea Gradients, and Conservation. *Current biology : CB* **27,** R511-R527; 10.1016/j.cub.2017.04.060 (2017).

19. Righetti, D., Vogt, M., Gruber, N., Psomas, A. & Zimmermann, N. E. Global pattern of phytoplankton diversity driven by temperature and environmental variability. *Science advances* **5,** eaau6253; 10.1126/sciadv.aau6253 (2019).

20. Chaudhary, C., Saeedi, H. & Costello, M. J. Bimodality of Latitudinal Gradients in Marine Species Richness. *Trends in ecology & evolution* **31,** 670–676; 10.1016/j.tree.2016.06.001 (2016).

21. Hirai, J., Tachibana, A. & Tsuda, A. Large-scale metabarcoding analysis of epipelagic and mesopelagic copepods in the Pacific. *PloS one* **15,** e0233189; 10.1371/journal.pone.0233189 (2020).

22. Lindsay, D. J. & Hunt, J. C. Biodiversity in midwater cnidarians and ctenophores: submersible-based results from deep-water bays in the Japan Sea and north-western Pacific. Submersible-based results from deep-water bays in the Japan Sea and north-western Pacific. *J. Mar. Biol. Ass.* **85,** 503–517; 10.1017/S0025315405011434 (2005).

23. Johnson, M. L., Shelton, P. M., Gaten, E. & Herring, P. J. Relationship of dorsoventral eyeshine distributions to habitat depth and animal size in mesopelagic decapods. *Biology Bulletin* **199,** 6–13 (2000).

24. Gjosaeter, J. & Kawaguchi, K. A review of the world resources of mesopelagic fish. Food and Agriculture Organization of the United Nation, 1980.

25. Moriarty, R. & O'Brien, T. D. Distribution of mesozooplankton biomass in the global ocean. *Earth Syst. Sci. Data* **5,** 45–55; 10.5194/essd-5-45-2013 (2013).

26. Steinberg, D. K., Cope, J. S., Wilson, S. E. & Kobari, T. A comparison of mesopelagic mesozooplankton community structure in the subtropical and subarctic North Pacific Ocean. *Deep Sea Research Part II: Topical Studies in Oceanography* **55,** 1615–1635; 10.1016/j.dsr2.2008.04.025 (2008).

27. Angel, M. V. Biodiversity of the Pelagic Ocean. *Conservation Biology* **7,** 760–772 (1993).

28. Brun, P., Payne, M. R. & Kiørboe, T. Trait biogeography of marine copepods - an analysis across scales. *Ecology letters* **19,** 1403–1413; 10.1111/ele.12688 (2016).

29. Vereshchaka, A., Abyzova, G., Lunina, A., Musaeva, E. & Sutton, T. A novel approach reveals high zooplankton standing stock deep in the sea. *Biogeosciences* **13,** 6261–6271; 10.5194/bg-13-6261-2016 (2016).

30. Ibarbalz, F. M. *et al.* Global Trends in Marine Plankton Diversity across Kingdoms of Life. *Cell* **179,** 1084-1097.e21; 10.1016/j.cell.2019.10.008 (2019).

31. Webb, T. J., Vanden Berghe, E. & O'Dor, R. Biodiversity's big wet secret: the global distribution of marine biological records reveals chronic under-exploration of the deep pelagic ocean. The global distribution of marine biological records reveals chronic under-exploration of the deep pelagic ocean. *PloS one* **5,** e10223; 10.1371/journal.pone.0010223 (2010).

32. Hidalgo, M. & Browman, H. I. Developing the knowledge base needed to sustainably manage mesopelagic resources. *ICES Journal of Marine Science* **76,** 609–615; 10.1093/icesjms/fsz067 (2019).

33. Dolan, R. J., Ritchie, E. M. & Rass, J. The ”neutral” community structure of planktonic herbivores, tintinnid ciliates of the microzooplankton, across the SE Tropical Pacific Ocean. *Biogeosciences Discussions, European Geosciences Union* **4,** 561–593 (2007).

34. Boltovskoy, D., Anderson, O. R. & Correa, N. M. Radiolaria and Phaeodaria. In *Handbook of the Protists,* edited by J. M. Archibald*, et al.* (Springer International Publishing, Cham, 2016), pp. 1–33.

35. Kosobokova, K. N., Hopcroft, R. R. & Hirche, H.-J. Patterns of zooplankton diversity through the depths of the Arctic’s central basins. *Mar Biodiv* **41,** 29–50; 10.1007/s12526-010-0057-9 (2011).

36. Palomares, M. & Pauly, D. *SeaLifeBase.www.sealifebase.org, version (04/2022).* (2022).

37. Reygondeau, G. Current and future biogeography of exploited marine groups under climate change. In *Predicting Future Oceans* (Elsevier2019), pp. 87–101.

38. Youden, W. J. Index for rating diagnostic tests **3,** 32–35; 10.1002/1097-0142(1950)3:1<32::AID-CNCR2820030106>3.0.CO;2-3 (1950).

39. Crisp, M. D., Laffan, S., Linder, H. P. & Monro, A. Endemism in the Australian flora. *J Biogeogr* **28,** 183–198; 10.1046/j.1365-2699.2001.00524.x (2001).

40. Pollock, L. J., Thuiller, W. & Jetz, W. Large conservation gains possible for global biodiversity facets. *Nature* **546,** 141–144; 10.1038/nature22368 (2017).

41. Burkenroad, M. D. The Templeton Crocker Expedition. XII. Sergestidae (Crustacea Decapoda) from the Lower Californian region, with descriptions of two new species and some remarks on the Organs of Pesta in Sergestes. *Zoologica, New York.* **22,** 315–329 (1937).

42. WoRMS. *llosergestes pestafer (Burkenroad, 1937). Accessed at: https://www.marinespecies.org/aphia.php?p=taxdetails&id=514113 on 2023-01-21* (2023).

43. Hobohm, C. *Endemism in vascular plants* (Springer, Dordrecht, 2014).

44. Boltovskoy, D., Correa, N. & Boltovskoy, A. Marine zooplanktonic diversity: a view from the South Atlantic. *Oceanologica Acta* **25,** 271–278; 10.1016/S0399-1784(02)01199-4 (2002).

45. Bucklin, A. *et al.* A “Rosetta Stone” for metazoan zooplankton: DNA barcode analysis of species diversity of the Sargasso Sea (Northwest Atlantic Ocean). *Deep Sea Research Part II: Topical Studies in Oceanography* **57,** 2234–2247; 10.1016/j.dsr2.2010.09.025 (2010).

46. Koplin, J. Community composition of epipelagic zooplankton in the Eurasian Basin 2017 determined by ZooScan image analysis. Thesis. University of Hamburg, 2020.

47. Jerez-Guerrero, M., Giraldo, A. & Criales-Hernandez, M. I. Temporal changes in the epipelagic copepod assemblage at Gorgona Island, Colombian Eastern Tropical Pacific Ocean. *REGIONAL STUDIES IN MARINE SCIENCE* **52**; 10.1016/j.rsma.2022.102280 (2022).

48. Drago, L. *et al.* Global Distribution of Zooplankton Biomass Estimated by In Situ Imaging and Machine Learning. *Front. Mar. Sci.* **9**; 10.3389/fmars.2022.894372 (2022).

49. Daniels, J., Sherman, A. D. & Katija, K. Illuminating gelatinous life in the deep sea. *Physics Today* **74,** 62–63; 10.1063/PT.3.4842 (2021).

50. Lebrato, M. *et al.* Sinking of Gelatinous Zooplankton Biomass Increases Deep Carbon Transfer Efficiency Globally. *Global Biogeochem. Cycles* **33,** 1764–1783; 10.1029/2019GB006265 (2019).

51. Rogers, A. D. *et al.* Discovering marine biodiversity in the 21st century. *Advances in marine biology* **93,** 23–115; 10.1016/bs.amb.2022.09.002 (2022).

52. Murphy, E. J. *et al.* Understanding the structure and functioning of polar pelagic ecosystems to predict the impacts of change. *Proceedings. Biological sciences* **283**; 10.1098/rspb.2016.1646 (2016).

53. Benedetti, F. *et al.* Major restructuring of marine plankton assemblages under global warming (vol 12, 5226, 2021). *Nature communications* **12**; 10.1038/s41467-021-26564-6 (2021).

54. Flessa, K. W. & Jablonski, D. Biogeography of recent marine bivalve molluscs and its implications for paleobiogeography and the geography of extinction: A progress report. *Historical Biology* **10,** 25–47; 10.1080/10292389509380512 (1995).

55. Beaugrand, G., Kirby, R. & Goberville, E. The mathematical influence on global patterns of biodiversity. *Ecology and evolution* **10,** 6494–6511; 10.1002/ece3.6385 (2020).

56. Hempel, G. On the biology of polar seas, particularly the Southern Ocean. *Marine biology of polar regions and effects of stress on marine organisms (J S Gray, M E Christiansen, eds) Wiley, Chichester* (1985).

57. Eastman, J. T. Comparison of the Antarctic and Arctic fish faunas. *Cybium (Paris)* **21,** 335–352 (1997).

58. Rohde, K. Latitudinal gradients in species diversity and their causes. II. Marine parasitological evidence for a time hypothesis. *Biol. Zbl.* **97,** 405–418 (1978).

59. Rohde, K. Latitudinal Gradients in Species Diversity: The Search for the Primary Cause. *Oikos* **65,** 514; 10.2307/3545569 (1992).

60. Evans, K. L., Greenwood, J. J. D. & Gaston, K. J. Dissecting the species-energy relationship. *Proc. R. Soc. B* **272,** 2155–2163; 10.1098/rspb.2005.3209 (2005).

61. Righetti, D., Vogt, M., Gruber, N. & Zimmermann, N. E. *Mapping global marine biodiversity under sparse data conditions* (2023).

62. Brown, H. J., Gillooly, J., Allen, P. A., van Savage, M. & West, B. G. Toward a metabolic theory of ecology. Ecology **85,** 1771–1789 (2004).

Supplemental Material

Table S1: Available databases of the environmental parameters used in this study.

Environmental variables	Unit	Data Source	Time period	Spatial resolution
Ocean Temperature (Temp)	°C	World Ocean Atlas 2018 https://www.ncei.noaa.gov/access/world-ocean-atlas-2018/bin/woa18.pl?parameter=t	Long-term annual mean (1981-2010)	1°
Salinity (Sal)	unitless	World Ocean Atlas 2018 https://www.ncei.noaa.gov/access/world-ocean-atlas-2018/bin/woa18.pl?parameter=s	Long-term annual mean (1981-2010)	1°
Mixed Layer Depth (MLD)	m	World Ocean Atlas 2018 https://www.ncei.noaa.gov/access/world-ocean-atlas-2018/bin/woa18.pl?parameter=M	Long-term annual mean (1981-2010)	1°
Dissolved Oxygen concentration (O_2)	$\mu mol \cdot kg^{-1}$	World Ocean Atlas 2018 https://www.ncei.noaa.gov/access/world-ocean-atlas-2018/bin/woa18oxnu.pl?parameter=o	annual mean	1°
Nitrate concentration (NO_3)	$\mu mol \cdot kg^{-1}$	World Ocean Atlas 2018 https://www.ncei.noaa.gov/access/world-ocean-atlas-2018/bin/woa18oxnu.pl?parameter=n	annual mean	1°
Net Primary Production (NPP)	$PgC \cdot m^{-3} \cdot year^{-1}$	GDFL ES2M	Long-term annual mean (1996-2015)	9 km
Euphotic Depth (Z_{eu})	m	Aqua/MODIS Level-3 Mapped Euphotic Depth Data Version 2018 https://hermes.acri.fr/index.php?class=archive	Long-term annual mean (1997-2022)	4 km

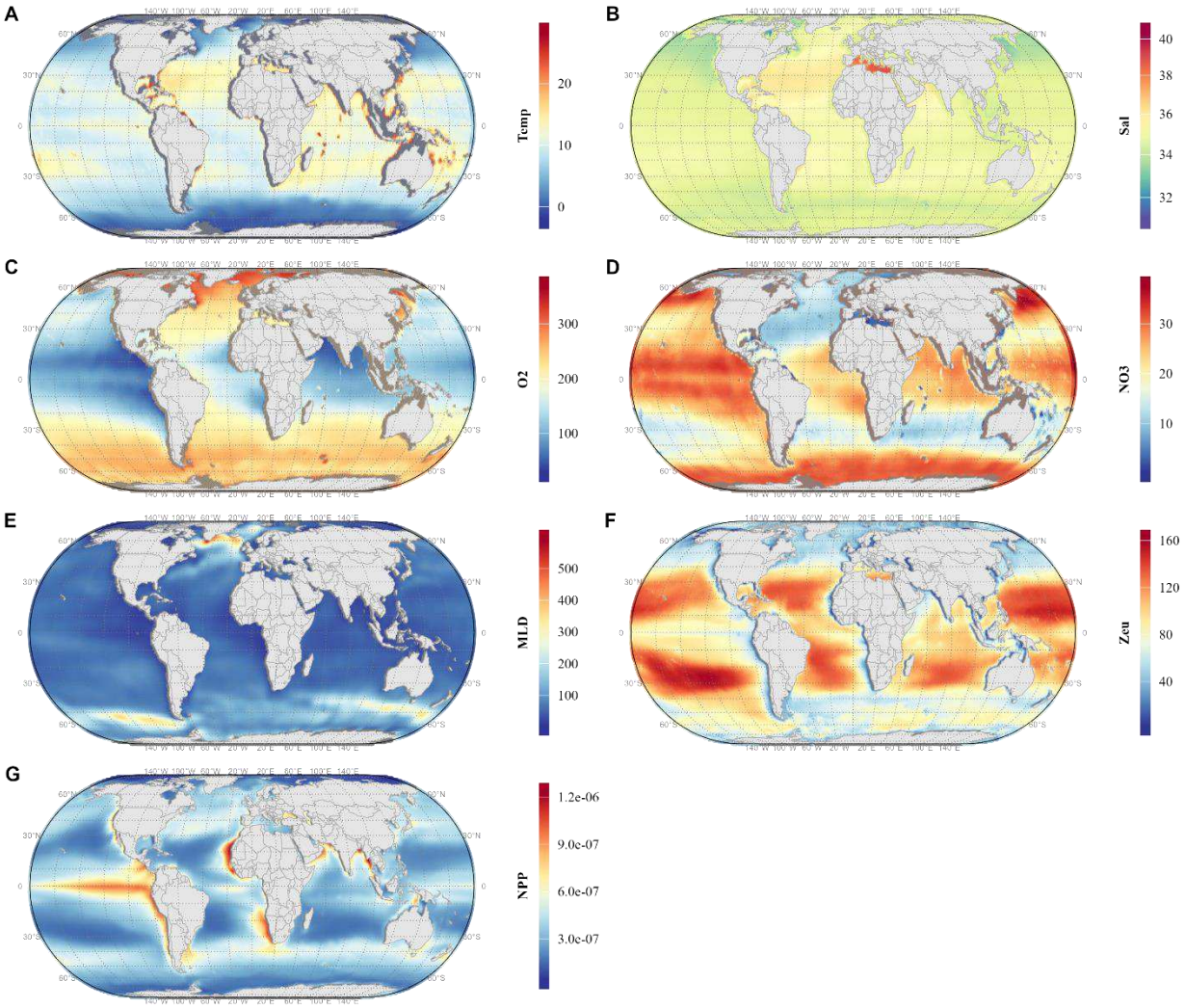

528

529 Figure S1: Distribution of annual climatology data in the mesopelagic layer for A) Temperature
530 (Temp, °C), B) Salinity (Sal, ‰), C) dissolved oxygen (O_2, µmol·kg^{-1}), D) dissolved nitrate (NO_3,
531 µmol·kg^{-1}), E) dissolved phosphate (PO_4, µmol·kg^{-1}), F) euphotic zone depth (Zeu, m), and G) Net
532 primary production (NPP, PgC·m^{-3}·yr^{-1}). All maps in Eckert IV global equal area projection.

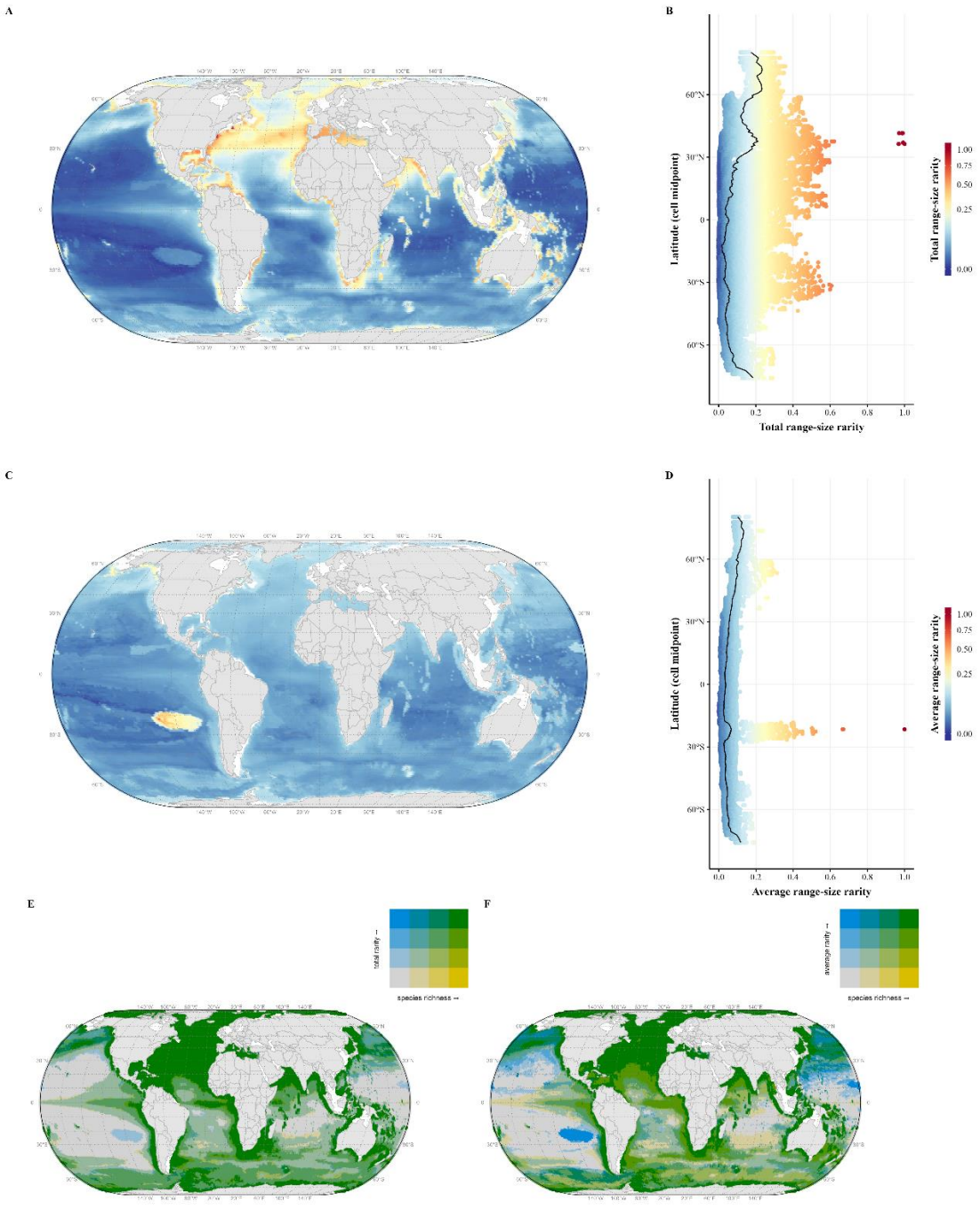

Figure S2: Average and total rarity plots using all species (n=861). A) Total range-size rarity map and B) latitudinal gradient for the total range-size rarity. A solid black line is a mean total range-size rarity per latitude. C) Average range-size rarity map and D) latitudinal gradient for the average range-size rarity. A solid black line is a mean total range-size rarity per latitude. E) 2D map depicting the relationship between the species richness and average total range-size rarity. F) 2D map depicting the relationship between the species richness and average total range-size rarity. For both maps E and F, quantile breaks were created at the 25th, 50th, and 75th percentiles. All maps in Eckert IV global equal area projection.

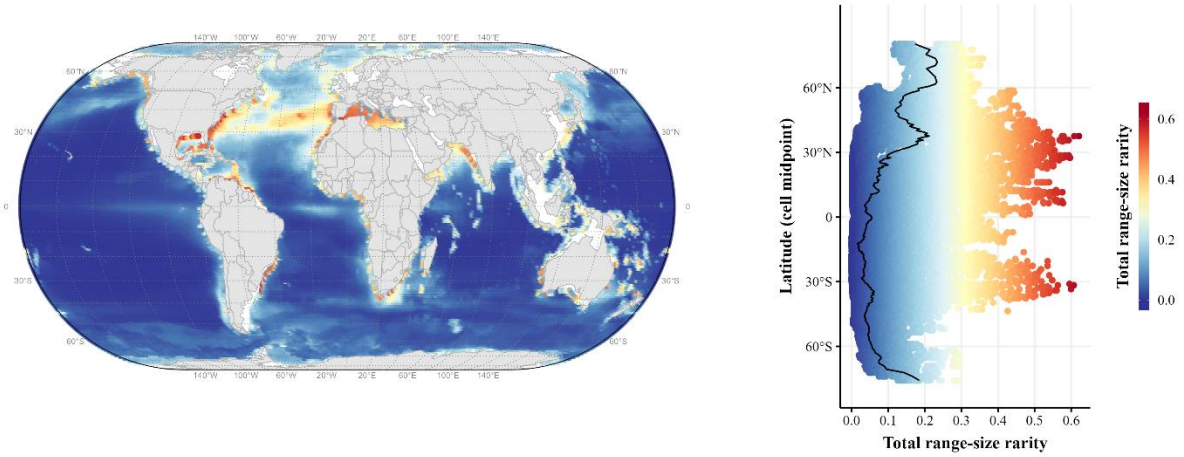

542

543 Figure S3: Filtered total range-size rarity map (rarity values >0.7 were removed; left) and
544 latitudinal gradient for the total range-size rarity (right). A solid black line is a mean total range-
545 size rarity per latitude. All maps in Eckert IV global equal area projection.

546

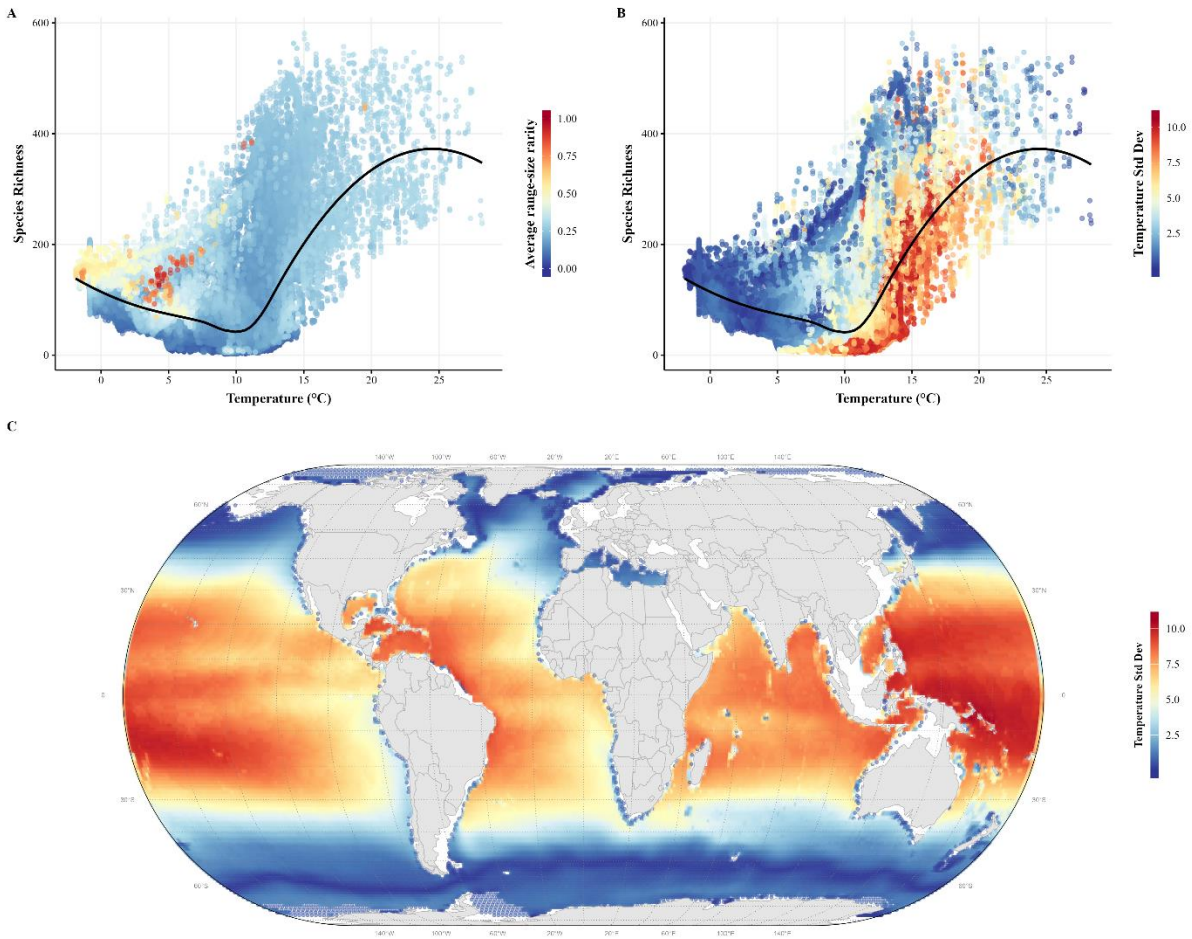

547

548 Figure S4: A) Relationship between the calculated species richness with the seawater temperature
549 of the mesopelagic layer colored by average rarity. Black line is loess-fitted line. B) Relationship
550 between the calculated species richness with the seawater temperature of colored by standard
551 deviation of climatological mean temperature (°C) in the mesopelagic layer. Black line is loess-
552 fitted line. C) Map showing the distribution of standard deviation of climatological mean
553 temperature (°C) in the mesopelagic layer in the mesopelagic zone. All maps are in Eckert IV
554 global equal area projection.

555

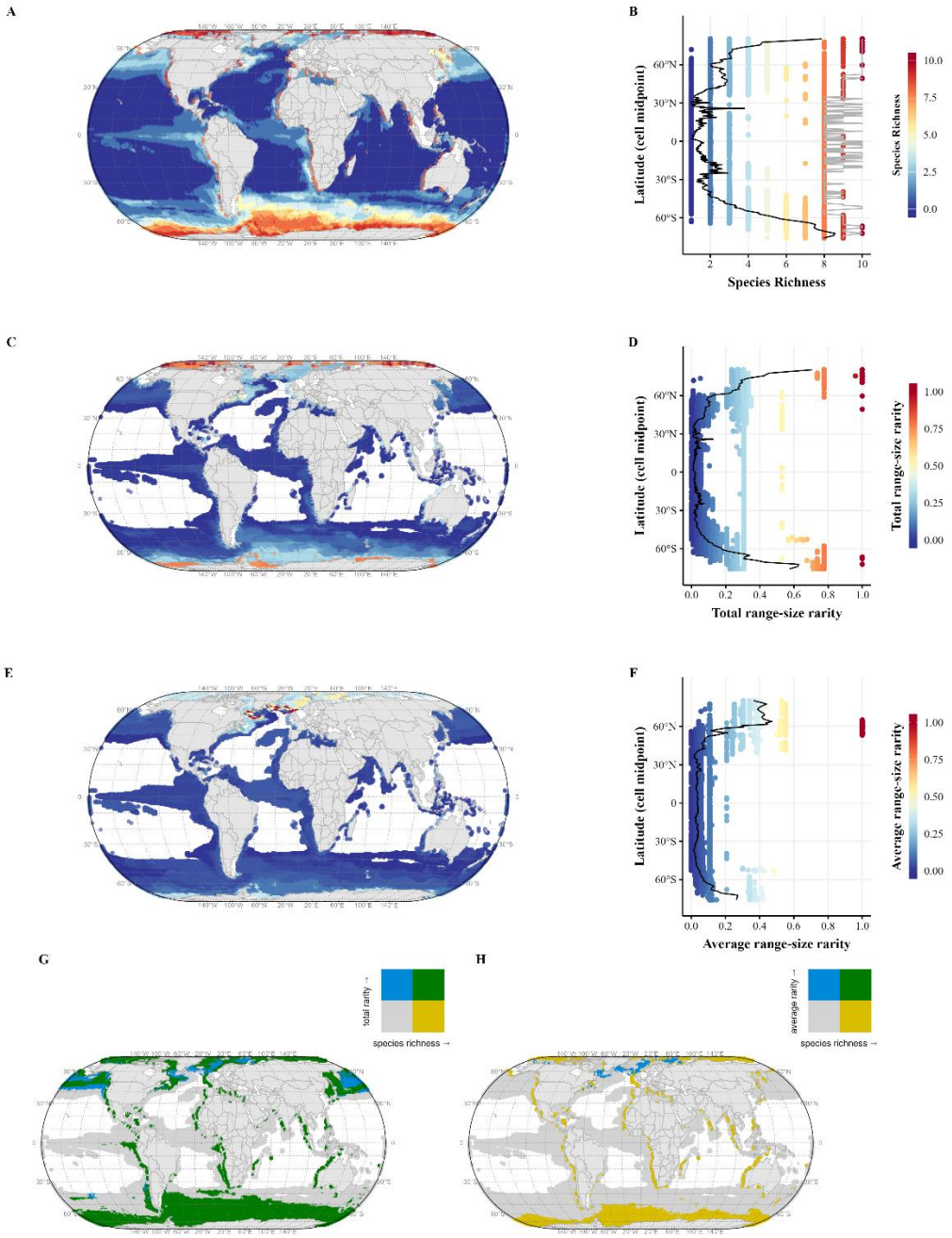

Figure S5: A) Mesopelagic Annelida species richness map (n=10). B) Latitudinal gradient showing mean (solid black line) and a number of unique species (grey solid line) per latitude. C) Total range-size rarity map and D) latitudinal gradient for the total range-size rarity. Solid black line is a mean total range-size rarity per latitude. E) Average range-size rarity map and F) latitudinal gradient for the average range-size rarity. Solid black line is a mean total range-size rarity per latitude. G) 2D map depicting the relationship between the species richness and average total range-size rarity. H) 2D map depicting the relationship between the species richness and average total range-size rarity. For both maps G and F, quantile breaks were created at the 50th percentile. All maps in Eckert IV global equal area projection.

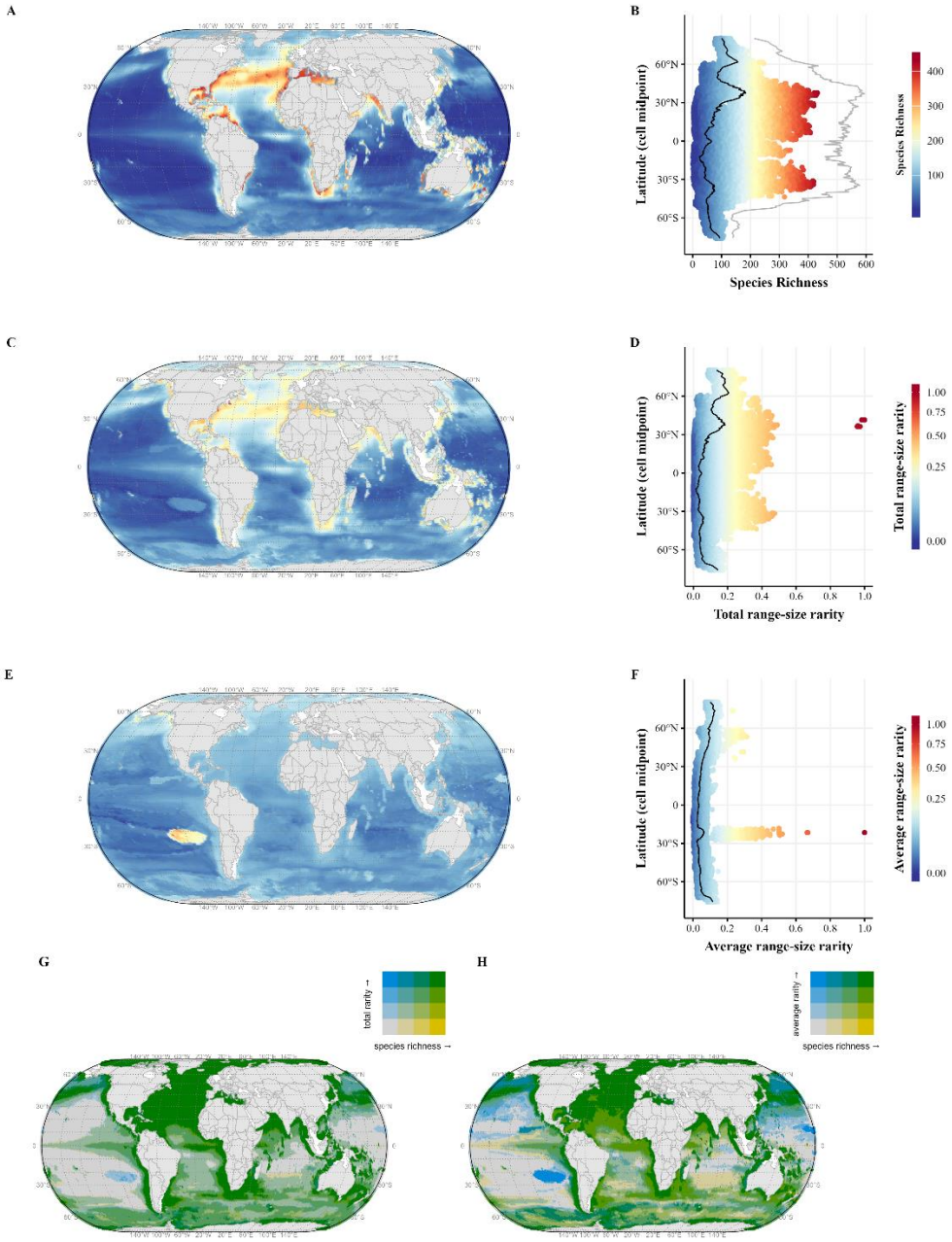

Figure S6: A) Mesopelagic Arthropoda species richness map (n=644). B) Latitudinal gradient showing mean (solid black line) and a number of unique species (grey solid line) per latitude. C) Total range-size rarity map and D) latitudinal gradient for the total range-size rarity. Solid black line is a mean total range-size rarity per latitude. E) Average range-size rarity map and F) latitudinal gradient for the average range-size rarity. Solid black line is a mean total range-size rarity per latitude. G) 2D map depicting the relationship between the species richness and average total range-size rarity. H) 2D map depicting the relationship between the species richness and average total range-size rarity. For both maps G and F, quantile breaks were created at the 25th, 50th, and 75th percentiles. Note, that square root transformation was applied to color scale in plots C-F for better interpretation. All maps in Eckert IV global equal area projection.

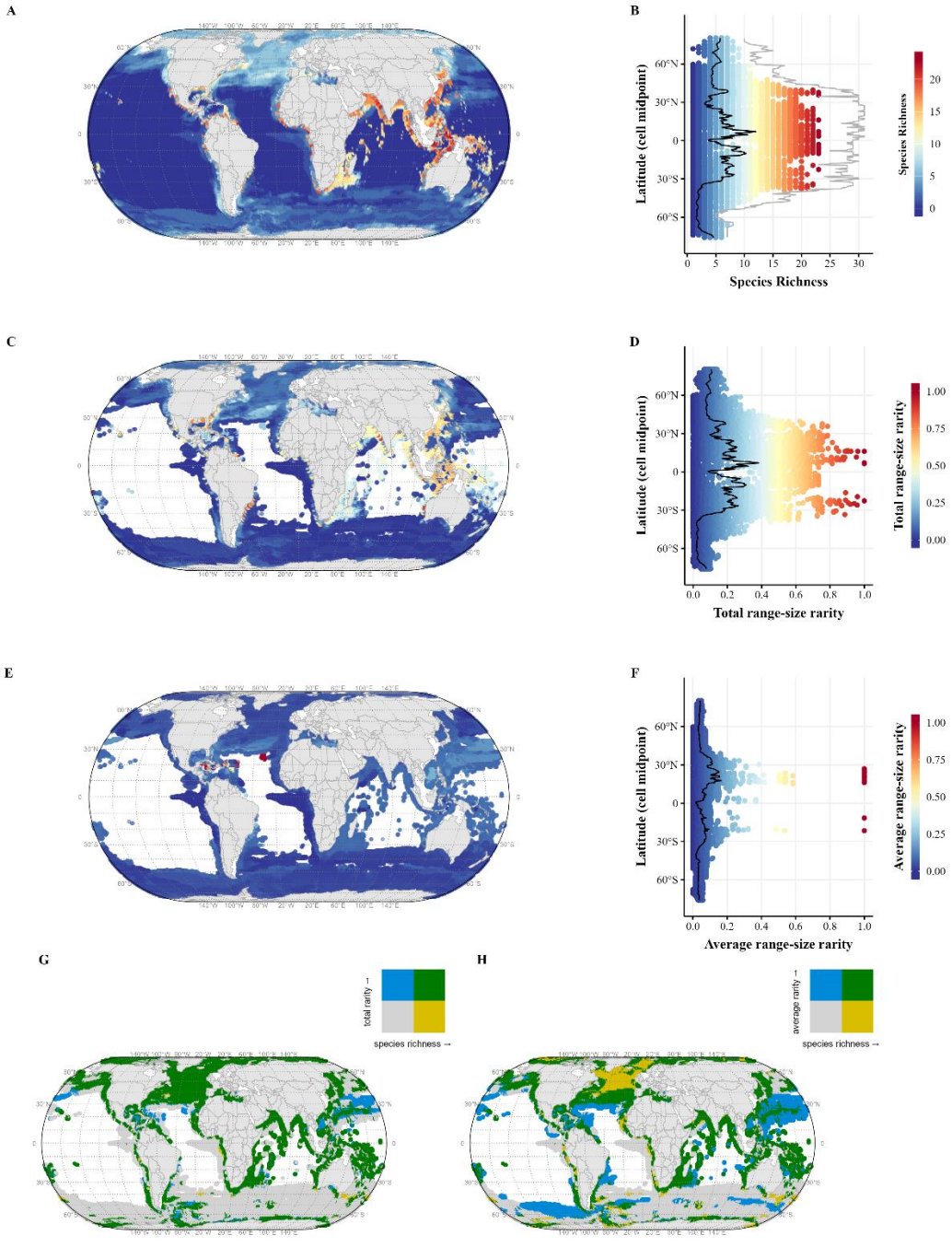

Figure S7: A) Mesopelagic Chaetognatha species richness map (n=31). B) Latitudinal gradient showing mean (solid black line) and a number of unique species (grey solid line) per latitude. C) Total range-size rarity map and D) latitudinal gradient for the total range-size rarity. Solid black line is a mean total range-size rarity per latitude. E) Average range-size rarity map and F) latitudinal gradient for the average range-size rarity. Solid black line is a mean total range-size rarity per latitude. G) 2D map depicting the relationship between the species richness and average total range-size rarity. H) 2D map depicting the relationship between the species richness and average total range-size rarity. For both maps G and F, quantile breaks were created at the 50th percentile. All maps in Eckert IV global equal area projection.

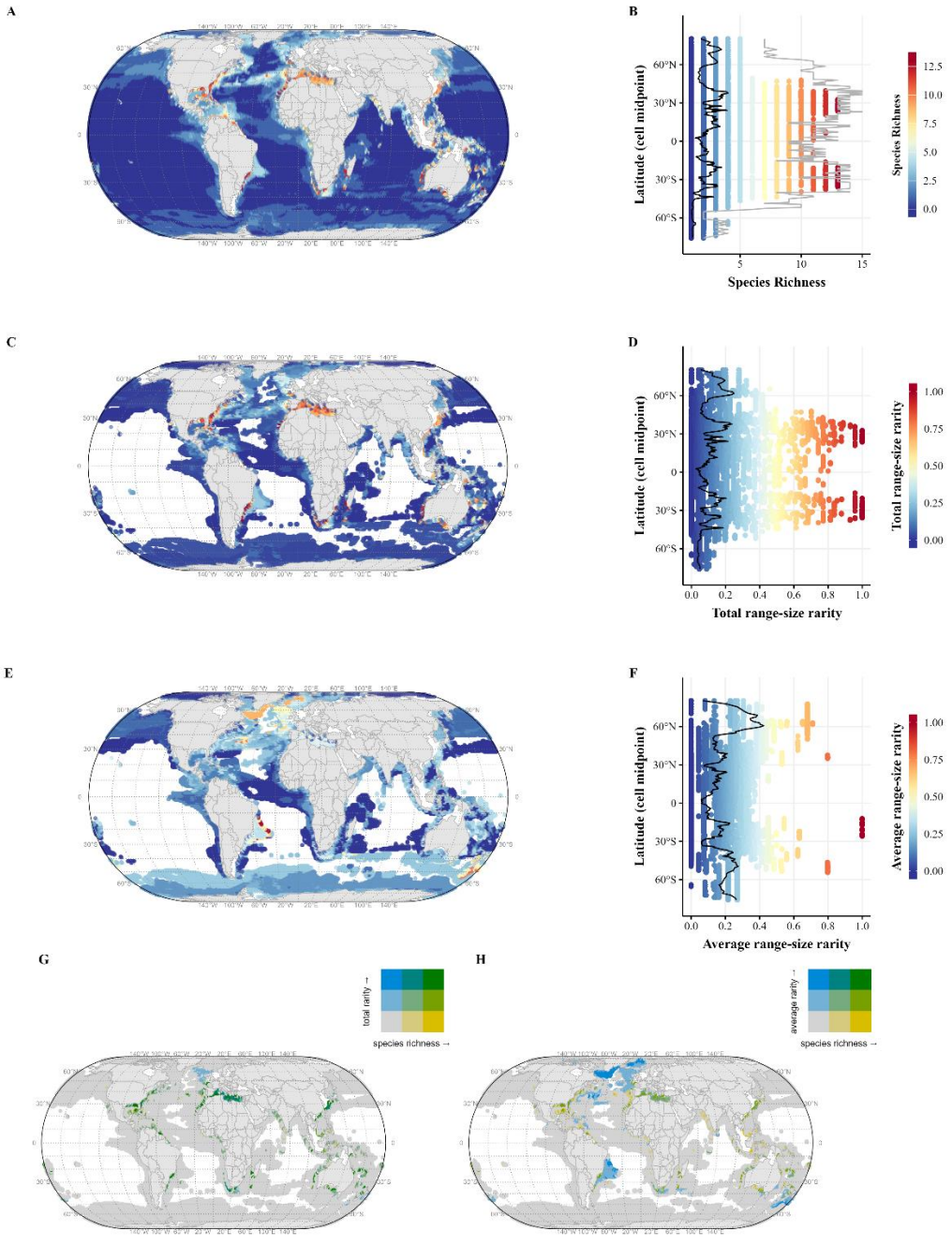

Figure S8: A) Mesopelagic Chordata species richness map (n=15). B) Latitudinal gradient showing mean (solid black line) and a number of unique species (grey solid line) per latitude. C) Total range-size rarity map and D) latitudinal gradient for the total range-size rarity. Solid black line is a mean total range-size rarity per latitude. E) Average range-size rarity map and F) latitudinal gradient for the average range-size rarity. Solid black line is a mean total range-size rarity per latitude. G) 2D map depicting the relationship between the species richness and average total range-size rarity. H) 2D map depicting the relationship between the species richness and average total range-size rarity. For both maps G and F, breaks were created by dividing mapping data into 3 equal intervals. All maps in Eckert IV global equal area projection.

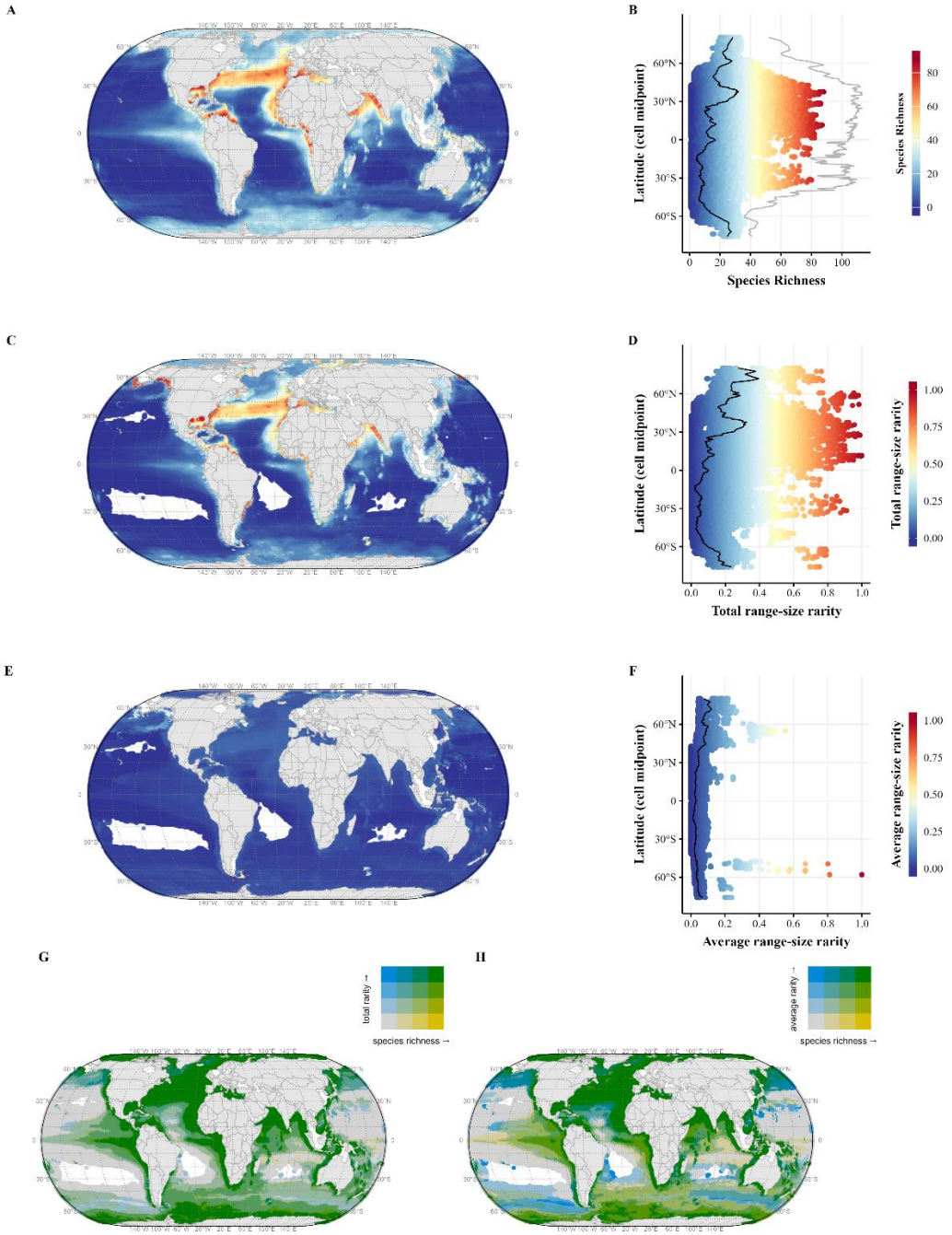

Figure S9: A) Mesopelagic Cnidaria species richness map (n=123). B) Latitudinal gradient showing mean (solid black line) and a number of unique species (grey solid line) per latitude. C) Total range-size rarity map and D) latitudinal gradient for the total range-size rarity. Solid black line is a mean total range-size rarity per latitude. E) Average range-size rarity map and F) latitudinal gradient for the average range-size rarity. Solid black line is a mean total range-size rarity per latitude. G) 2D map depicting the relationship between the species richness and average total range-size rarity. H) 2D map depicting the relationship between the species richness and average total range-size rarity. For both maps G and F, quantile breaks were created at the 25th, 50th, and 75th percentiles. All maps in Eckert IV global equal area projection.

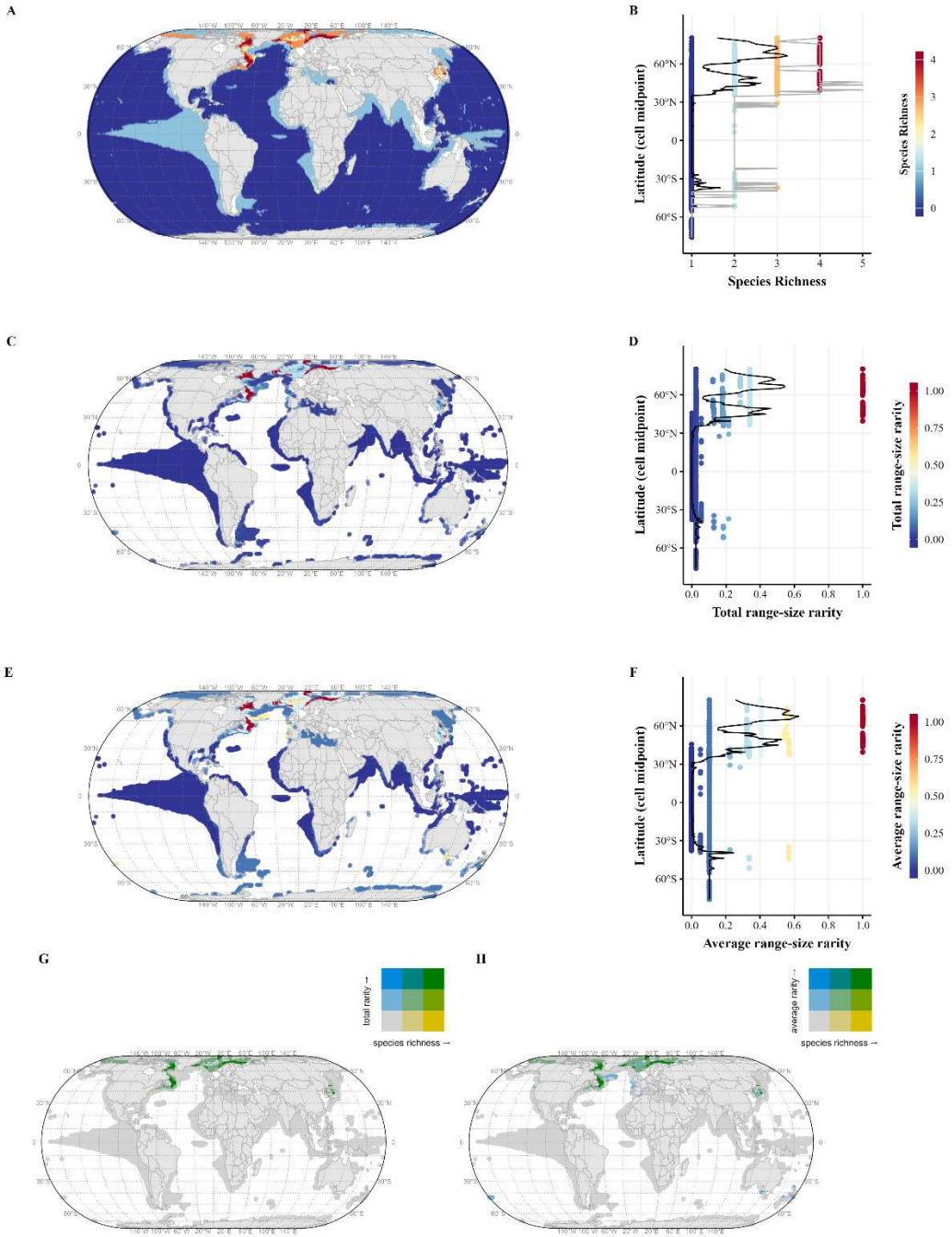

Figure S10: A) Mesopelagic Ctenophora species richness map (n=8). B) Latitudinal gradient showing mean (solid black line) and a number of unique species (grey solid line) per latitude. C) Total range-size rarity map and D) latitudinal gradient for the total range-size rarity. Solid black line is a mean total range-size rarity per latitude. E) Average range-size rarity map and F) latitudinal gradient for the average range-size rarity. Solid black line is a mean total range-size rarity per latitude. G) 2D map depicting the relationship between the species richness and average total range-size rarity. H) 2D map depicting the relationship between the species richness and average total range-size rarity. For both maps G and F, quantile breaks were created by dividing mapping data into 3 equal intervals. All maps in Eckert IV global equal area projection.

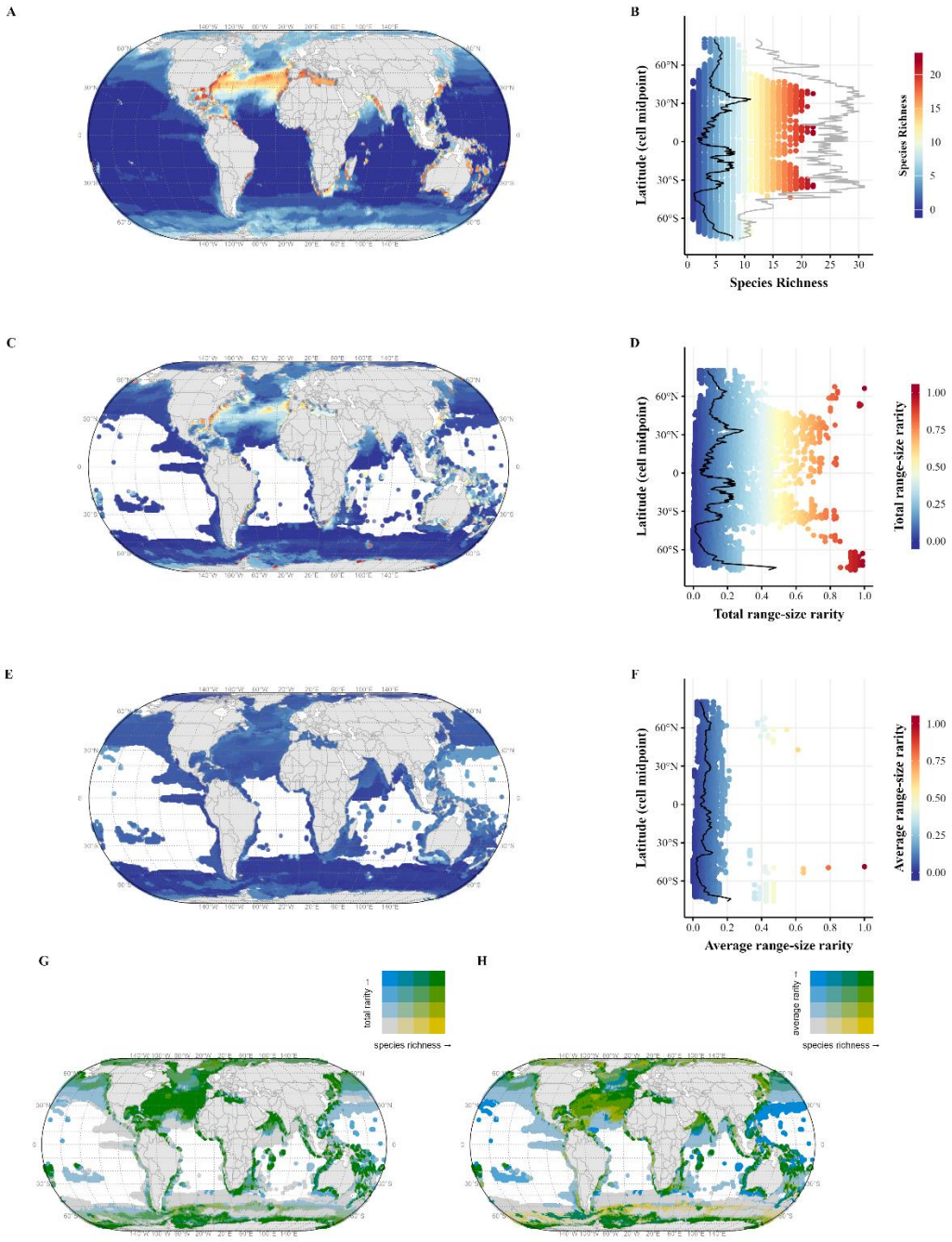

Figure S11: A) Mesopelagic Mollusca species richness map (n=33). B) Latitudinal gradient showing mean (solid black line) and a number of unique species (grey solid line) per latitude. C) Total range-size rarity map and D) latitudinal gradient for the total range-size rarity. Solid black line is a mean total range-size rarity per latitude. E) Average range-size rarity map and F) latitudinal gradient for the average range-size rarity. Solid black line is a mean total range-size rarity per latitude. G) 2D map depicting the relationship between the species richness and average total range-size rarity. H) 2D map depicting the relationship between the species richness and average total range-size rarity. For both maps G and F, quantile breaks were created at the 25th, 50th, and 75th percentiles. All maps in Eckert IV global equal area projection.

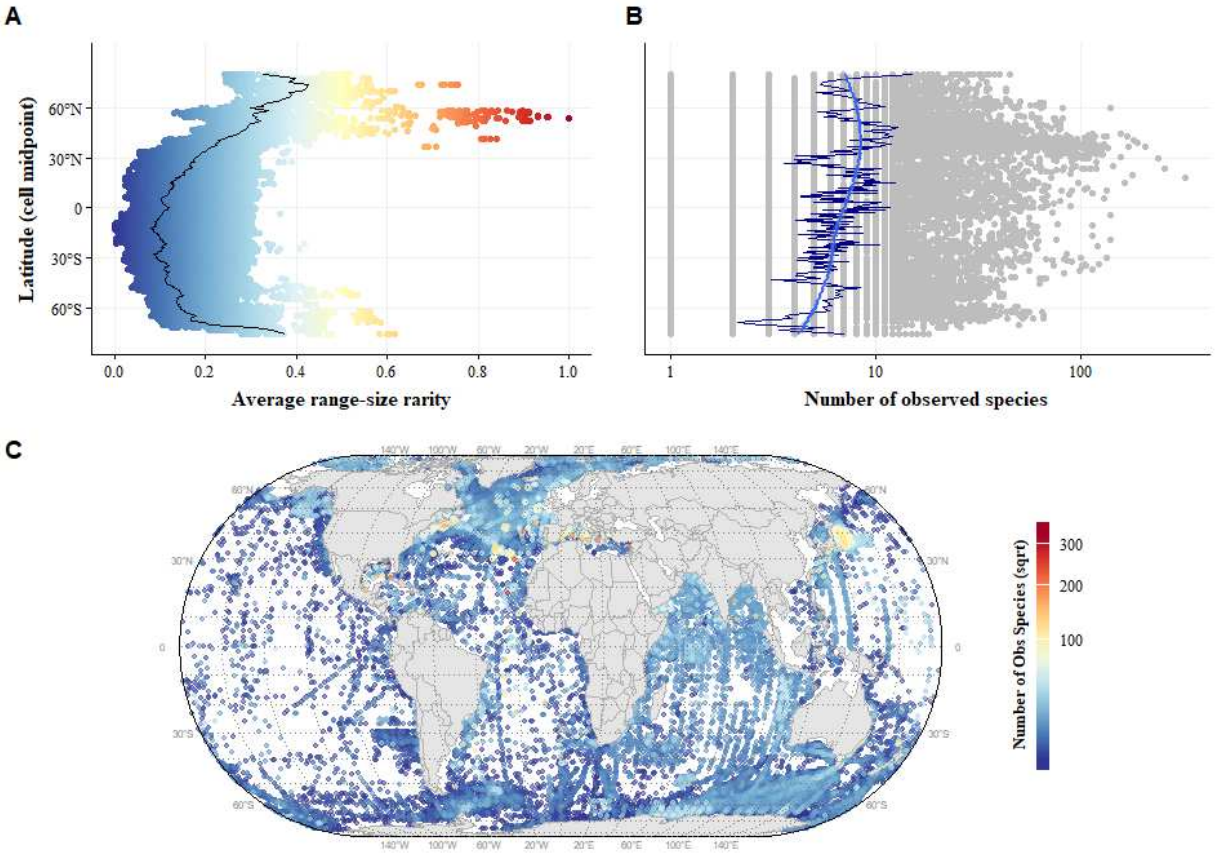

627

628 Figure S12: Sampling effort. A) latitudinal gradient of average range-size rarity in relation to the
629 distribution of B) number of observed species and black line is a mean value per latitude, blue line
630 is a fitted loess line. C) Sampling effort showing number of species recorded in each cell. All maps
631 in Eckert IV global equal area projection.

Supplementary Files

This is a list of supplementary files associated with this preprint. Click to download.

- rs.pdf